Supporting information

SI materials and methods

SEC analysis. To assay the interaction between various forms of Vac8 and Vac17, protein samples (10–20 μM final protein concentration) were prepared in 20 mM Tris-HCl pH 7.5, 150 mM NaCl, and 5 mM dithiothreitol at 4°C. Proteins were applied to a HiLoad 16/60 Superdex 200 pg column (GE Healthcare). Molecular mass standards comprising ferritin (440 kDa), aldolase (158 kDa), conalbumin (75 kDa), ovalbumin (44 kDa), carbonic anhydrase (29 kDa), and ribonuclease A (13.7 kDa) were used for calibration. The eluted protein samples were subjected to SDS-PAGE followed by Coomassie Brilliant Blue staining.

Pull-down assay. For the His_6-tag pull-down assay shown in Figure 1A, supernatants from *E. coil* cells expressing various truncated Vac17 proteins (His_6-SUMO-fusion) were mixed with 10 μL Ni-NTA agarose beads (Qiagen, Germany) for 1 h at 4°C. After incubation, beads were washed three times with buffer B (25 mM sodium phosphate pH 7.4, 400 mM sodium chloride, 50 mM imidazole, 0.1% Triton X-100, and 0.1% NP-40) and then mixed with 100 μg purified wild-type or mutant Vac8 proteins in a total volume of 600 μL. The assay mixture was incubated at 4°C for 60 min, and beads were washed three times with 600 μL buffer B. Proteins were eluted with SDS sample buffer and subjected to 12% SDS-PAGE. For the experiment presented in Figure 5C, supernatants of *E. coli* cells co-expressing GST-Vac8 (residues 1–39); Vac8 (residues 40–578); and His_6-tagged tVac17, Nvj1, or Atg13 were incubated with 10 μL Ni-NTA agarose beads for 1 h at 4°C. The beads were washed three times with buffer B, and then proteins were analyzed by 15% SDS-PAGE. For the GST pull-down assay shown in Figure 2C and Supplementary Figure S5C, supernatants of *E. coli* cells expressing wild-type or mutant GST-Vac8 (residues 1–578) were incubated with Glutathione Sepharose 4B beads (GE Healthcare) for 1 h at 4°C. Beads were washed twice with buffer A and mixed with 100 μg Halo-tag-fused tVac17, $Nvj1^{229\text{-}321}$, and $Atg13^{567\text{-}695}$ proteins for 1 h at 4°C. The

mixtures were washed again three times with buffer A, and proteins were analyzed by 12% SDS-PAGE.

ITC analysis. For ITC experiments, protein samples (sample cell: 0.05 mM, syringe: 0.7 mM) indicated in Figures 2D and 4B were prepared in buffer C (25 mM Tris-HCl pH 7.5, 150 mM NaCl, and 4 mM β-mercaptoethanol). ITC measurements were performed using a Microcal ITC200 instrument (Malvern Panalytical, UK) at 25°C. Measurements were taken over 20 injections of 2 µL sample with a reference power of 5 µcal/s and at a stirring speed of 1000 rpm. The data were fitted using MicroCal PEAQ-ITC analysis software (Malvern Panalytical) with a 1:1 binding model.

Induction of Cvt. Cells were inoculated in YPD medium and grown overnight at 30°C in a shaking incubator. Thereafter, cells were diluted to an OD_{600} of 0.1 in YPD medium containing FM 4-64 (1 µM) and incubated at 30°C for 1 h. Finally, cells were collected by centrifugation (3,000 ×g) at room temperature for 1 min, resuspended in fresh YPD or SD-N medium, and further grown at 30°C for 3 h.

Protein extraction from yeast cells and immunoblotting. Yeast cells were grown in YPD medium overnight and collected by centrifugation (3,000 ×g) at room temperature for 1 min when OD_{600} had reached 1.5–2.0. Thereafter, cells were resuspended in 0.1 mL PBS and 0.1 mL of 2× SDS-PAGE sample buffer and mixed with 0.1 mL glass beads (0.5 mm diameter; BioSpec, Bartlesville, OK, USA) for cell lysis. After three cycles of boiling and vortexing (1 min each), cell lysates were recovered by centrifugation (room temperature, 1 min, 10,000 ×g). Protein extracts were analyzed by SDS-PAGE followed by immunoblotting using anti-Vac8, anti-myc (Cell Signaling Technology, Danvers, MA, USA), and anti-Act1 antibodies.

Coimmunoprecipitation. Yeast spheroplasts were prepared as described (1), resuspended in ice-cold solubilization buffer (25 mM Tris-Cl, pH 7.4, 150 mM NaCl, 1%

NP-40, 1 mM EDTA, 5% glycerol, 1 mM PMSF, and 10 mM leupeptin), and incubated on ice for 20 min. Detergent-insoluble material was removed by centrifugation at 16,200 × *g* (10 min, 4°C). The resulting post-centrifugation supernatants were precleared by incubation with protein A Sepharose (GE Healthcare) at 4°C for 1 h. Anti-myc antibodies, control mouse IgG, anti-GFP antibodies, or control rabbit IgG were added to the precleared supernatants and incubated at 4°C on a nutator mixer for 5 h. Protein A Sepharose was then added and further incubated for 1 h. Protein A Sepharose beads were collected by centrifugation at 3,000 × *g* (1 min, 4°C) and washed three times with ice-cold solubilization buffer. Bound proteins were eluted with SDS sample buffer for SDS-PAGE analysis followed by immunoblotting using anti-myc and anti-GFP antibodies.

Supplementary figures

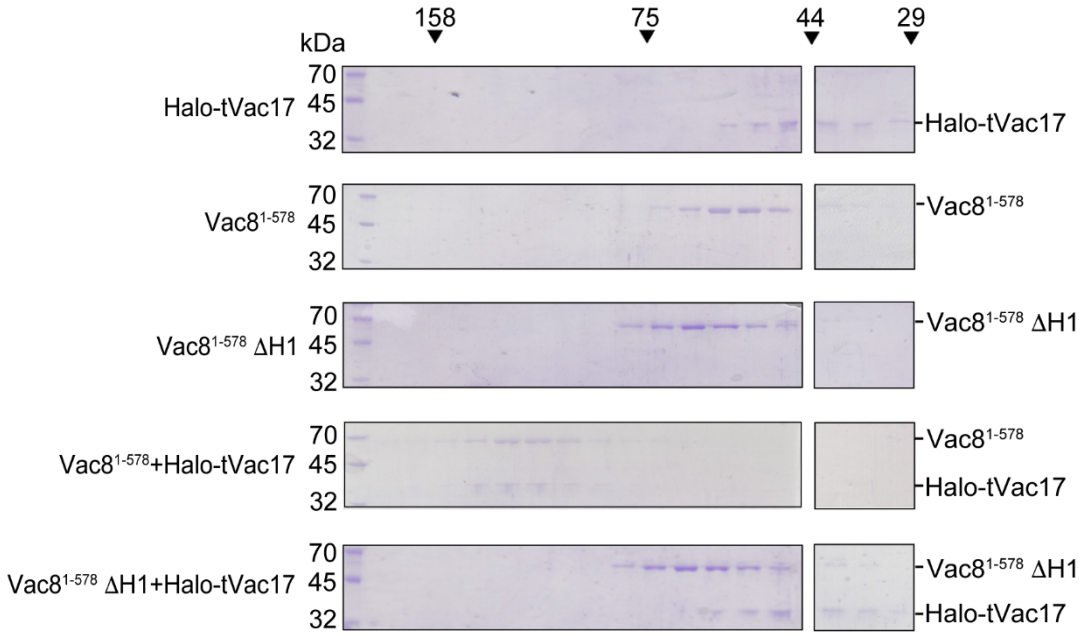

Supplementary Figure S1. SDS-PAGE shows the eluted protein fractions separated by SEC shown in Figure 1B. The standard molecular masses are shown above the gels.

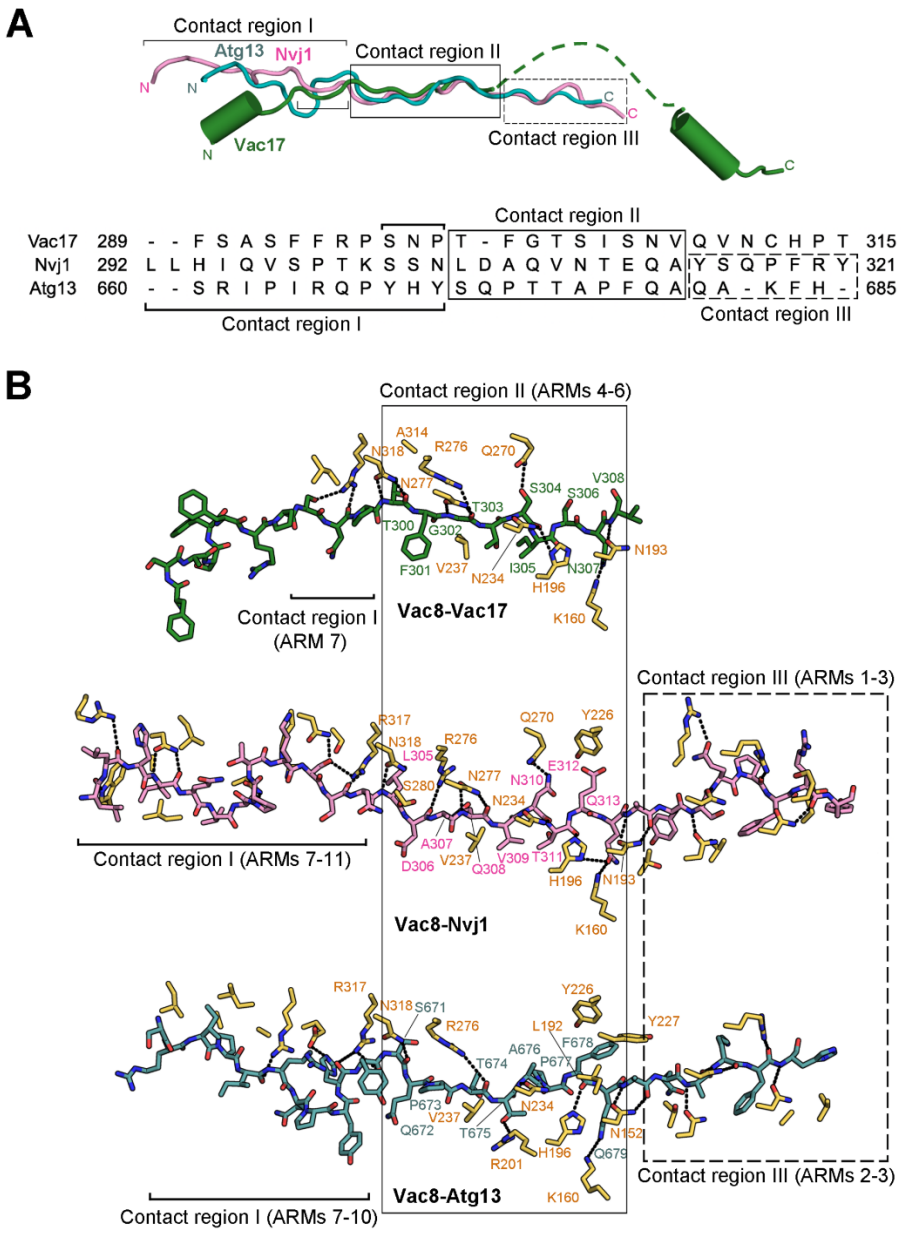

Supplementary Figure S2. Structural comparison of Vac17, Atg13, and Nvj1 in complex with Vac8. (A) Ribbon representation showing the superposition of Vac17 (green), Nvj1 (pink), and Atg13 (teal) bound to tVac8. Based on structural conservation, contact sites between Vac8 and its binding partners are divided and highlighted. The sequence alignment of *S. cerevisiae* Vac17, Nvj1, and Atg13 is shown below. (B) Comparison of the interactions between the central ARM domain of Vac8 (yellow/orange) and its binding peptides Vac17 (green), Nvj1 (pink), and Atg13 (teal). Oxygen and nitrogen

atoms are colored red and blue, respectively. Black dotted lines indicate intermolecular hydrogen bonds.

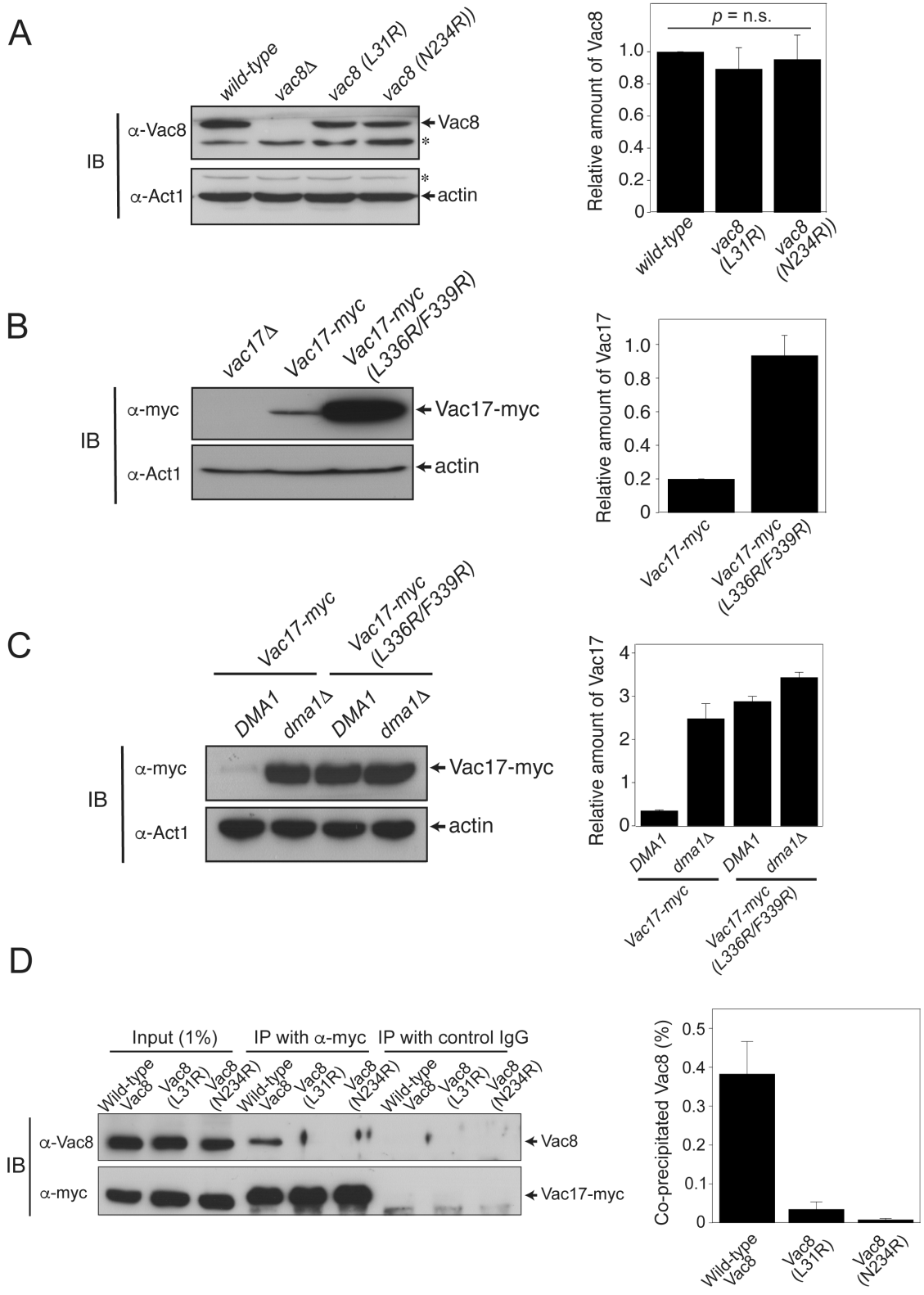

Supplementary Figure S3. Comparable expression of wild-type Vac8 and Vac17 versus mutant Vac8 and Vac17. (A) Expression of wild-type Vac8, Vac8(L31R), and Vac8(N234R) was analyzed by immunoblotting. The expression level of Vac8 proteins was normalized to that of actin and quantified in the bar graph on the right. Data represent the means ± SEM (error bars; n = 3). p = n.s. Tukey's test. Asterisks indicate non-specific bands. (B) Expression of myc-tagged wild-type Vac17 or Vac17 (L336R/F339R) in *vac17*Δ yeast cells was analyzed by immunoblotting. Actin was used as a loading control. The expression level of Vac17 proteins was normalized to that of actin and quantified in the bar graph on the right. Data represent the means ± SEM (error bars; n = 3). (C) The Vac17 (L336R/F339R) mutant, defective for Vac8 binding, is more resistant than wild-type Vac17 to Dma1-mediated ubiquitinylation followed by proteasomal degradation. The expression of myc-tagged wild-type Vac17 or Vac17 (L336R/F339R) in *DMA1*/*vac17*Δ or *dma1*Δ/*vac17*Δ yeast cells was analyzed by immunoblotting. Actin was used as a loading control. (D) The L31R or N234R mutation of Vac8 largely abolishes the interaction between Vac8 and Vac17-myc. Yeast spheroplasts were detergent-solubilized, and detergent-insoluble material was removed by centrifugation. The resulting post-centrifugation supernatants were precleared by incubation with protein A Sepharose and treated with anti-myc antibodies or control mouse IgG. Protein A Sepharose was then added, and bound proteins were eluted with SDS sample buffer for SDS-PAGE analysis followed by immunoblotting with anti-myc and anti-Vac8 antibodies.

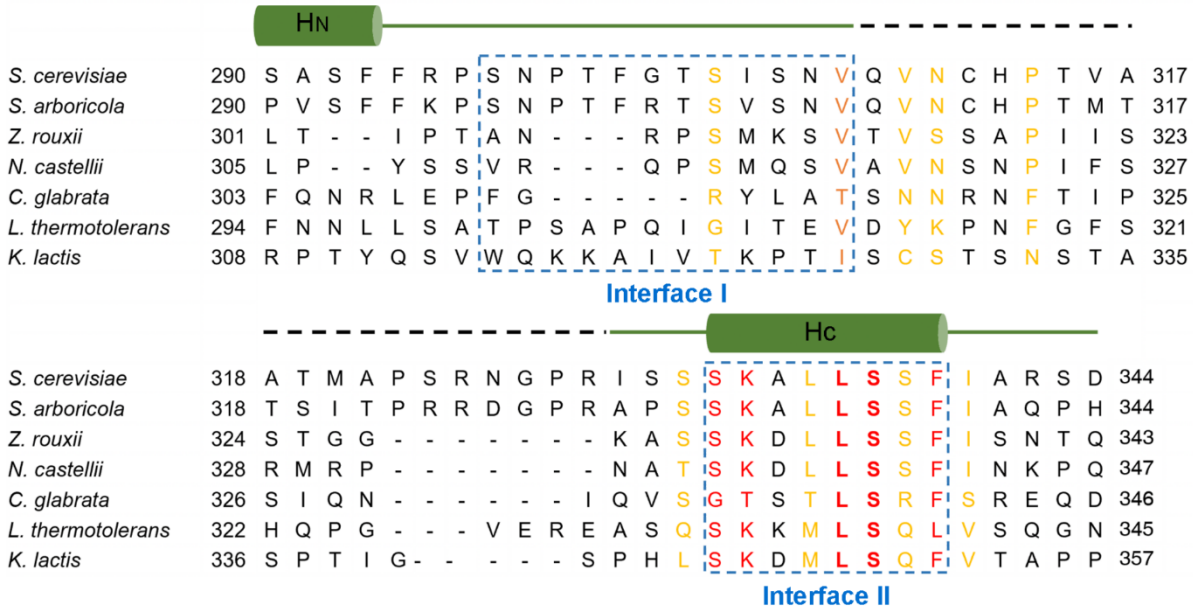

105

106 **Supplementary Figure S4. Sequence alignment of tVac17 (Vac8-binding domain) from**
107 **seven species.** Sequence alignment of tVac17 from *S. cerevisiae* (UniProt entry: P25591),
108 *S. arboricola* (UniProt entry: J8PR22), *Z. rouxii* (C5DZ63), *N. castelli* (G0VAW8), *C.*
109 *glabrata* (Q6FX71), *L. thermotolerans* (C5DJZ0), and *K. lactis* (Q6CV25). Secondary
110 structural elements based on the crystal structure are shown above the sequence by
111 green cylinders (α-helices), green lines (loops), and black dashed lines (disordered
112 regions). Sequence conservation at each amino acid is represented by a color gradient
113 from yellow (70% identity) to bold red (100% identity). The Vac8-binding interfaces
114 (Interfaces I and II) are marked by blue dashed boxes.

115

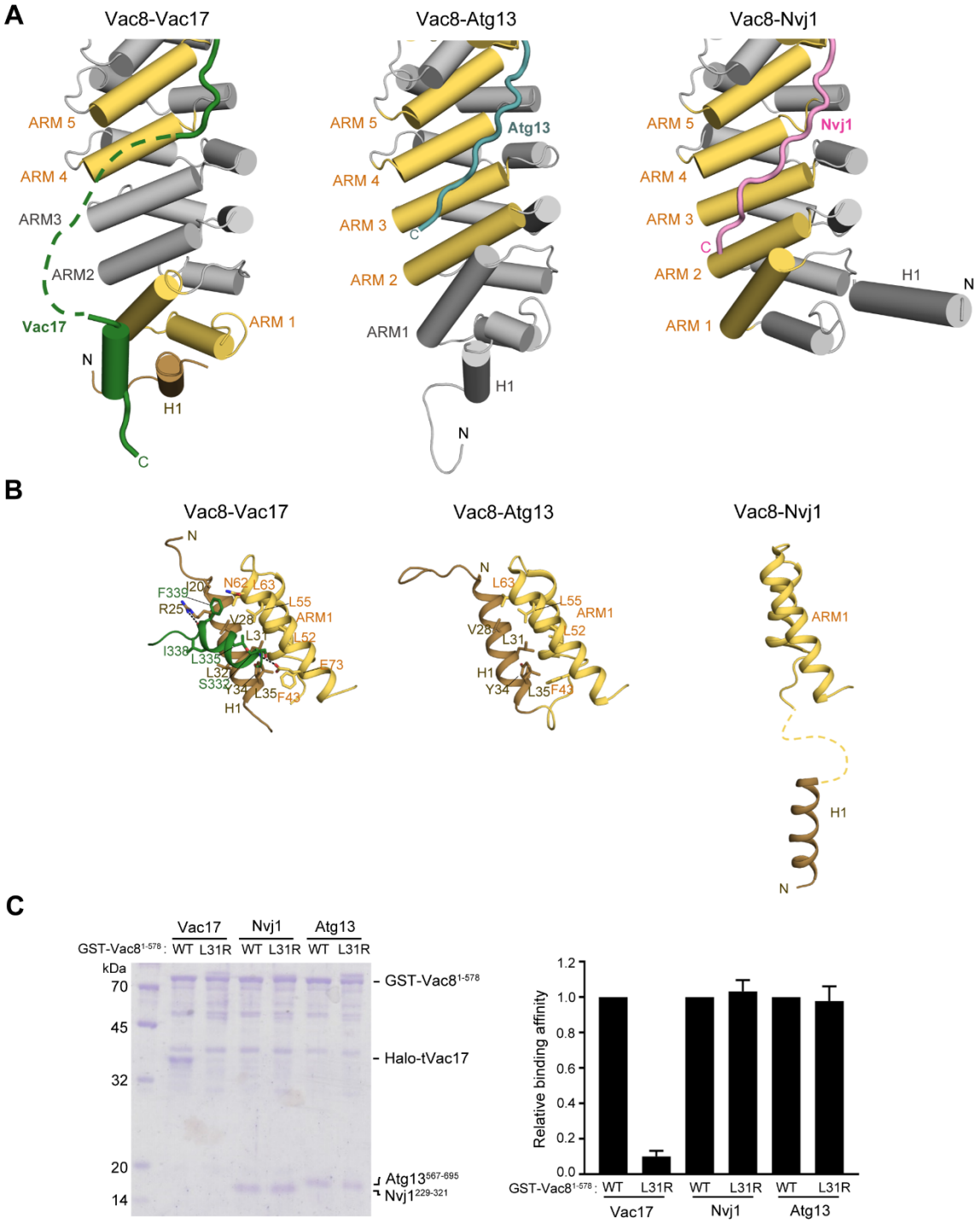

116

117 **Supplementary Figure S5. Dynamic organization of the H1 helix of Vac8.** (A) Cartoon
118 representation structurally comparing the Vac8 H1 helix when Vac8 interacts with the
119 Vac17, Atg13, or Nvj1 peptide. The ARM repeat helices involved in the interaction with
120 peptides are highlighted in yellow. The H1 helix is colored brown. (B) Ribbon diagrams

comparing the structural conformation of ARM1 (H2 and H3 helices) and the H1 helix of Vac8 between the Vac8-Vac17, Vac8-Atg13, and Vac8-Nvj1 complexes. In the Vac8-Vac17 complex, the Hc helix of Vac17 directly contacts both the H1 helix and ARM1 of Vac8. (C) GST pull-down experiments using wild-type Vac8 and the mutant Vac8 (L31R) show that the H1 helix of Vac8 is required for interaction with Vac17 but not with Nvj1 or Atg13. The pull-down results are quantified in the bar graph on the right (n=3).

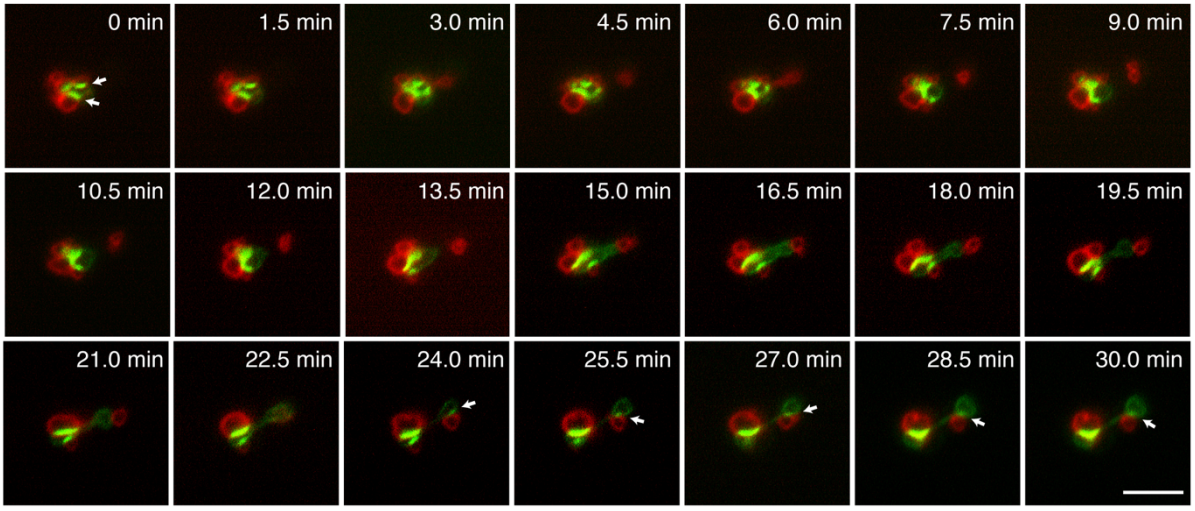

Supplementary Figure S6. Live imaging of yeast cells undergoing mitosis revealed that preformed NVJs in mother cells remain largely intact during vacuole segregation into daughter cells. Yeast cells expressing Nvj1-EGFP were stained with FM 4-64, and NVJs and organelle inheritance were analyzed by fluorescence microscopy. Images were taken every 1.5 min for 30 min, and images of a representative yeast cell are shown. White arrows indicate NVJs. Scale bar: 5 μm.

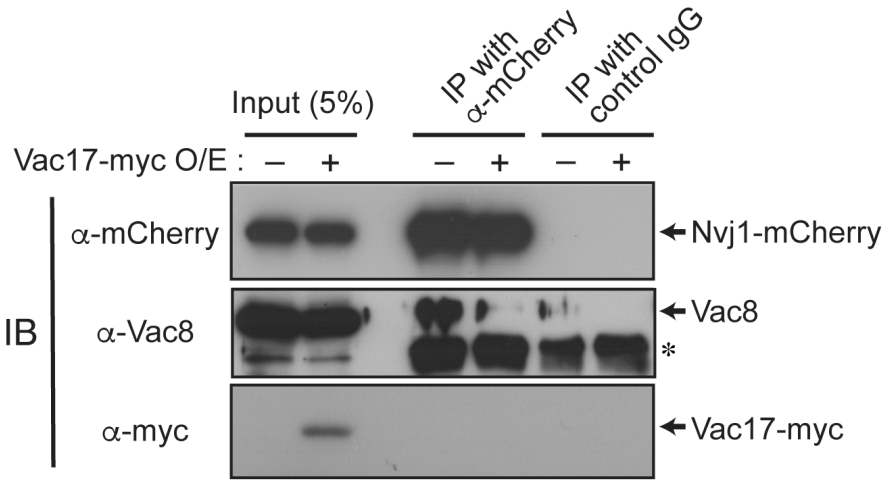

Supplementary Figure S7. Vac17 over-expression (O/E) inhibits the Vac8-Nvj1 interaction. Yeast spheroplasts were prepared from yeast cells expressing Nvj1-mCherry with or without overexpression of Vac17-myc from the *GPD1* promoter (see Supplementary Table S3 for details of yeast strains used). The spheroplasts were detergent-solubilized, and detergent-insoluble material was removed by centrifugation. The resulting post-centrifugation supernatants were precleared by incubation with protein A Sepharose and treated with anti-mCherry antibodies or control rabbit IgG. Protein A Sepharose was then added, and bound proteins were eluted with SDS sample buffer for SDS-PAGE analysis followed by immunoblotting with anti-Vac8, anti-myc, or anti-mCherry antibodies. The asterisk indicates non-specific (IgG heavy chain) signals from the immunoprecipitating antibodies.

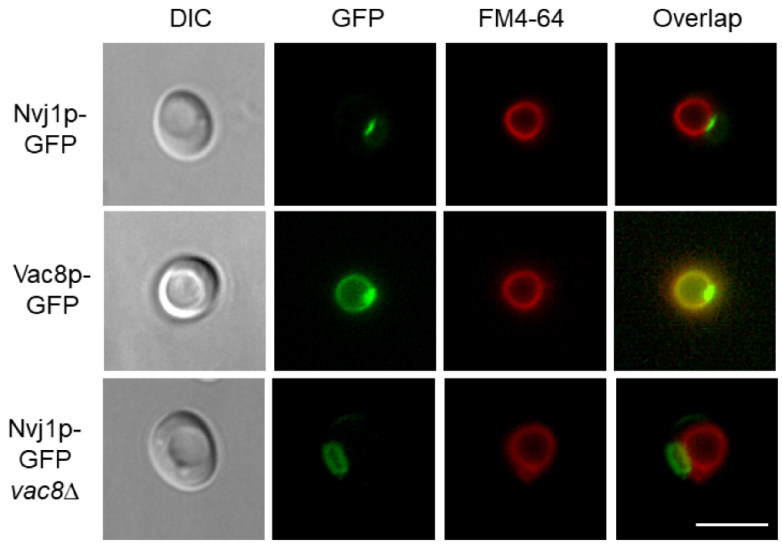

Supplementary Figure S8. The majority of Nvj1 seems to exist in Vac8-Nvj1 complexes, but free Vac8 exists along the vacuolar membrane as a binding platform for various proteins, including Atg13 and Vac17. Scale bar: 5 μm.

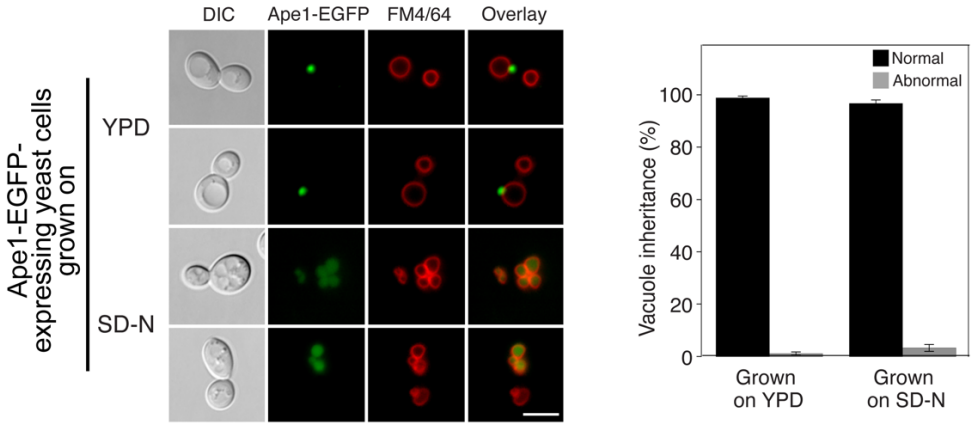

Supplementary Figure S9. Vacuole inheritance and Cvt can occur simultaneously. Yeast cells expressing Ape1p-EGFP were grown in the presence of FM 4-64 at 30°C for 1 h. Cells were then collected, resuspended in fresh YPD or SD-N medium, and further incubated at 30°C for 3 h. Ape1p-EGFP and FM 4-64 were analyzed by fluorescence microscopy. Representative images are shown (left) (scale bar: 5 μm), and bar graphs show the quantification of vacuole inheritance (right). More than 100 cells per strain were examined in each experiment. Data represent the means ± SEM (error bar; n=3).

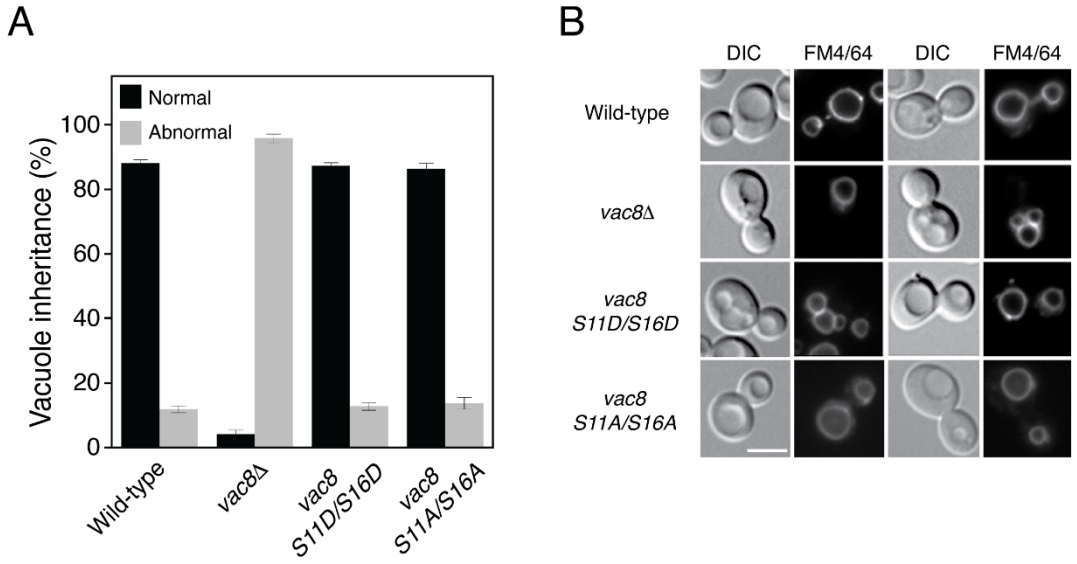

163

164 **Supplementary Figure S10.** Phosphorylation/dephosphorylation of Ser11 and Ser16 in
165 Vac8 does not seem critical for vacuole inheritance. (A) Wild-type, vac8Δ,
166 phosphorylation-mimetic mutant Vac8 (S11D/S16D), and phosphorylation-defective
167 mutant Vac8 (S11A/S16A) cells were stained with FM 4-64 and their vacuole inheritance
168 was analyzed by fluorescence microscopy. More than 100 cells per strain were
169 examined in each experiment. Data represent the means ± SEM (error bar; n=3). (B)
170 Representative images are shown. Scale bar: 5 μm.

171

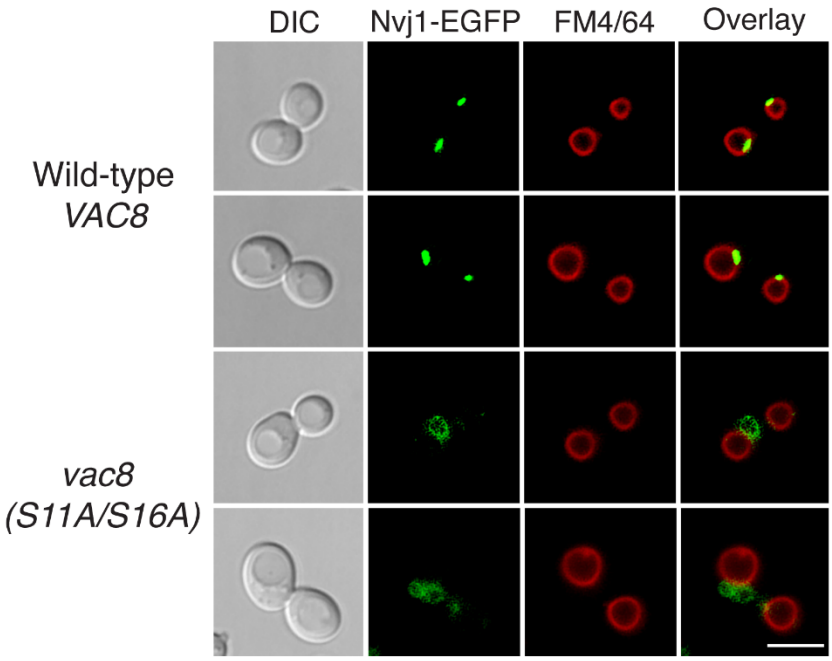

Supplementary Figure S11. Alanine substitutions of Ser11 and Ser16 of Vac8 block the formation of NVJs. Yeast cells expressing Nvj1-EGFP were treated with FM 4-64, and GFP fluorescence indicating NVJs and FM 4-64 fluorescence indicating vacuoles were analyzed by fluorescence microscopy (magnification: 100×). DIC, differential interference contrast.

Supplementary Table S1. Data collection and refinement statistics

	tVac8-tVac17
Dataset	Native
X-ray source	Beamline 5C, PAL
Temperature (K)	100
Space group:	I422
Cell parameters	
a, b, c (Å)	147.446, 147.446, 121.514
α, β, γ (°)	90.000, 90.000, 90.000
Data processing	
Wavelength (Å)	0.99190
Resolution (Å)	50.00–2.10
CC1/2	0.999 (0.365)
I/σ	27.2 (2.48)
Completeness (%)	99.6 (99.5)
Redundancy	9.5 (5.9)
Measured reflections	368,865
Unique reflections	38,976
Refinement statistics	
Resolution (Å)	36.86–2.10
Reflections	38,971
Number of atoms	
Protein	4008
Water	191
R-factor (%)	18.75
R_{free} (%)	22.33
RMSD	
Bond lengths (Å)	0.006
Bond angles (°)	0.907
Ramachandran plot, residues in	
Favored regions (%)	99.81
Allowed regions (%)	0.19
Disallowed regions (%)	0.00

*The highest resolution shell is shown in parentheses.

Supplementary Table S2. ITC thermograms summarizing the measured thermodynamic parameters

[Syringe] : [Cell]	K_d (mM)	N	ΔH (kJ mol^{-1})	-TDS (kJ mol^{-1})
[Halo] : [Vac8]	NB	-	-	-
[Halo-tVac17] : [Vac8]	2.53	0.963 ± 0.023	-14.5 ± 0.610	-17.5
[Halo-tVac17] : [Vac8^{L318R}]	NB	-	-	-
[Halo-tVac17] : [Vac8^{N214S}]	NB	-	-	-
[Halo-tVac17$^{L134R/F139R}$] : [Vac8]	NB	-	-	-
[Halo-tVac17] : [Vac8-Atg13$^{467-665}$]	NB	-	-	-
[Atg13$^{467-695}$] : [Vac8-tVac17]	9.02	0.239 ± 0.053	-22.2 ± 6.89	-6.63
[Halo-tVac17] : [Vac8-Nvj1$^{229-321}$]	NB	-	-	-
[Nvj1$^{229-321}$] : [Vac8-tVac17]	10.00	0.05 ± 0.133	-335 ± 944	306

Supplementary Table S3. Yeast strains used in this study

Strain	Genotype	Reference
BY4742	MATα *his3Δ1 leu2Δ0 lys2Δ0 ura3Δ0*	(2)
BY4742 *vac8Δ*	BY4742 *vac8Δ::KanMX4*	This study
BY4742 *vac17Δ*	BY4742 *vac17Δ::KanMX4*	This study
BY4742 *VAC8 (L31R)*	BY4742 *vac8Δ* with *pRS406-VAC8 (L31R)*	This study
BY4742 *VAC8 (N234R)*	BY4742 *vac8Δ* with *pRS406-VAC8 (N234R)*	This study
BY4742 *VAC17-myc*	BY4742 *vac17Δ* with *pYJ403-VAC17-myc*	This study
BY4742 *VAC7(L336R,F339R)*	BY4742 *vac17Δ* with *pYJ403-VAC17 (L336R,F339R)-myc*	This study
BY4742 *Ape1-EGFP*	BY4742 with *pYJ408-Ape1-EGFP*	This study
BY4742 *Vac8-EGFP/Vac8-myc*	BY4742 *vac8Δ* with *pYJ406-Vac8-EGFP and pYJ408-Vac8-myc*	(3)
BY4742 Vac8/Vac8/Vac17	BY4742 *Vac8-EGFP/Vac8-myc* with *pYJ403-Vac17-myc*	This study
BY4742 Nvj1-mCherry	BY4742 with *pYJ406-Nvj1-mCherry*	This study
BY4742 Nvj1/Vac17	BY4742 *Nvj1-mCherry* with *pYJ403-Vac17-myc*	This study

References

1. M. Cabrera, C. Ungermann, Purification and in vitro analysis of yeast vacuoles. *Methods Enzymol* **451**, 177-196 (2008).
2. E. A. Winzeler *et al.*, Functional characterization of the S. cerevisiae genome by gene deletion and parallel analysis. *Science* **285**, 901-906 (1999).
3. H. Jeong *et al.*, Mechanistic insight into the nucleus-vacuole junction based on the Vac8p-Nvj1p crystal structure. *Proc Natl Acad Sci U S A* **114**, E4539-E4548 (2017).